

Control of Self-excited Vibrations in Smooth and Non-smooth Systems

Department of Automation, Biomechanics and Mechatronics, Łódź University of Technology, Stefanowskiego Str. 1/15, 90-924 Łódź, Poland

jan.awrejcewicz@p.lodz.pl

Department of Mechanical Engineering, Amrita School of Engineering, Amrita Vishwa Vidyapeetham, Coimbatore 641 112, India

Abstract. In many engineering scenarios, self-excited vibrations lead to undesirable results. Aeroelastic flutter, machine-tool chatter and flow-induced instability of structures are some well-known examples. Such vibrations are typically characterised by robust attracting limit cycles which makes their control a difficult task. This article outlines different strategies for the control of undesirable selfexcited vibrations in smooth and non-smooth engineering systems. The control of flow-induced vibration by using parametric excitation in structure elasticity is demonstrated first. It is shown that the amplitude jump due to internal resonance between the wake and the structure in the lock-in region can be mitigated by parametric excitation. Parametric excitation leads to the formation of newer internal resonance regions which can be made to fall outside the original lock-in region by tuning the frequency ratio. Recent work on control of flow induced vibration using bistable nonlinear energy sink is outlined next. The bistable sink suppresses internal resonance in lock-in region and outperforms cubic sinks in control performance. BNES partitions the lock-in region into chaotic and non-chaotic subregions with an amplitude jump between the two. The article next deals with the control of non-smooth friction-induced vibration. The suppression of stick-slip oscillations in a three degree-of-freedom disc brake model is outlined. The discontinuity induced bifurcation responsible for this suppression is also illustrated and discussed.

Keywords: Self-excited Vibration · Vibration Control · Parametric Excitation

1 Introduction

Self-excited oscillations are very common in natural and engineering systems. The heart may be considered a self-excited oscillator and there have been various efforts, old and new, to arrive at self-excited models of human heart [1, 2]. Self-excited models have also found extensive applications in neuroscience [3]. Self-excitation also plays a very important role in the physics of bowed and wind musical instruments [4].

Perhaps the most well-known instance of self-excited oscillation in engineering is the collapse of the suspension bridge over the Tacoma Narrows in Washington in 1940. It is an example of self-excited vibration caused by flow-induced instability which has been studied extensively since [5]. This example also brings to focus the need for robust strategies to control self-excited vibrations. Flutter of aircraft wings is another well-known and dangerous example of self-excited vibration [6]. Machine tool chatter has also been recognised long since as an example of self-excited vibration [7]. Self-excited vibrations also happen in non-smooth systems. Friction induced vibrations in vehicle braking systems and in other types of contact problems serve as important examples [8].

Self-excited oscillations can be dangerous in many engineering situations (like wing flutter and flow-induced instability) and calls for efficient control strategies. Devising such strategies is a difficult task because of the robustness of self-excited vibrations due to the presence of highly stable attracting limit cycles. A systematic effort to develop a general theory of control of self-excited oscillations was made by Ales Tondl and his co-workers. Their strategy was based on the use of parametric excitation to quench self-excited vibration [9]. Subsequent work showed that complete quenching of self-excited oscillations can be brought about by tuning the frequency of parametric excitation [10]. Tondl called such suppression parametric anti-resonance and derived frequency conditions pertaining to it [11].

Other strategies have also been proposed to control self-excited oscillations in different scenarios. Nonlinear energy sink (NES) has been shown to be effective in controlling flow induced vibration [12]. It has also been demonstrated that NES fitted with a type of quadratic damping mechanism can be used to control self-excited vibrations in fluid carrying pipes [13]. Dohnal and Tondl [14] have also used parametric inertia excitations to control flutter. The possibility of controlling machine tool chatter by using parametric excitation has also been experimentally demonstrated [15].

Control mechanisms for self-excited oscillations in non-smooth systems have also been proposed. Delayed feedback mechanisms have become popular for the control of friction induced vibrations [16]. It has also been shown that low amplitude, high frequency forces, sometimes called dither, given normal to the direction of the frictional force can be an effective way to suppress friction induced vibrations [17].

In this article we outline recent work on strategies for the control of self-excited vibration in smooth and non-smooth systems. In Sect. 2, we demonstrate the ability of parametric excitation to control vortex induced vibrations. This section generalises Tondl's idea to the control of flow induced instabilities. We use flow induced vibration model with acceleration coupling and introduce parametric excitation in primary structure stiffness. Section 3 outlines recent work on the use of bistable nonlinear energy sink (BNES) to control self-excited flow induced vibrations. It is shown that BNES leads to vibration suppression in the lock-in region and that it outperforms the purely cubic NES. Recent work on control of non-smooth self-excited vibration is outlined in Sect. 4. Normal harmonic excitation is used to suppress stick-slip vibrations in a three degree-of-freedom disc brake model. Some important conclusions regarding vibration control in self-excited systems are drawn in Sect. 5.

2 Control of Flow Induced Vibration Using Parametric Excitation

The dimensionless governing equations for flow induced vibration are given by the following coupled second order ODEs [18]

$$\ddot{y} + \left(2\zeta\delta + \frac{\gamma}{\mu}\right)\dot{y} + \delta^2 y = Mq \tag{1}$$

$$\ddot{q} + \varepsilon \left(q^2 - 1\right)\dot{q} + q = A\ddot{y} \tag{2}$$

Equation (1) corresponds to the linear structure and Eq. (2) corresponds to the wake oscillator. Here, ζ is the structure damping, δ denotes the natural frequency of the structure, γ is the stall parameter, μ is a dimensionless mass ratio, M is essentially a coupling coefficient that scales the effect of the wake on the structure. In the wake oscillator equation, $\varepsilon \in [0, 1]$ is a small parameter and A is the acceleration coupling coefficient. For the parameter values $\zeta = 0.0031$, $\gamma = 0.8$, M = 0.0002, $\varepsilon = 0.3$, A = 12 and $\delta = 1$, the change of structural amplitude with the reduced velocity $U_r = \frac{1}{St.\delta}$ is given in Fig. 1. Here, St. is the Strouhal number with the value St. = 0.2.

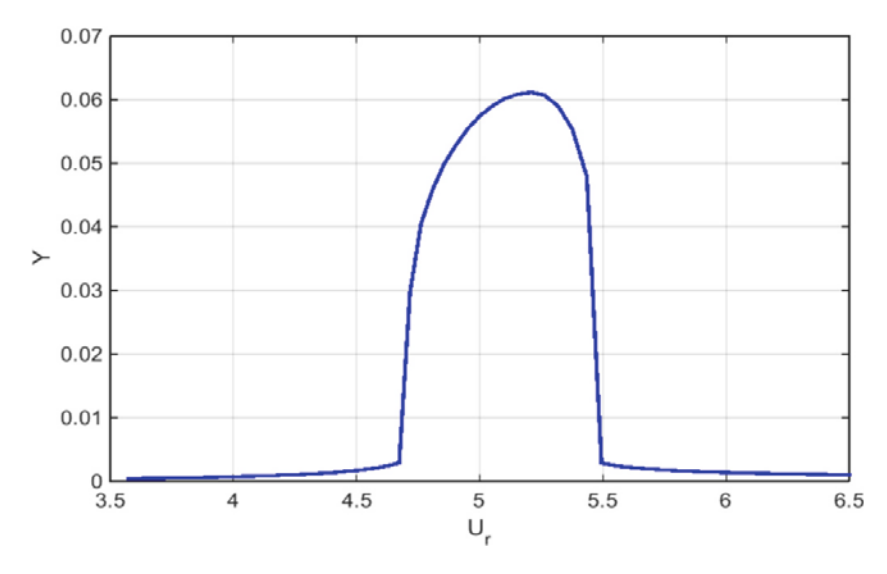


Fig. 1. Variation in structural amplitude as a function of reduced velocity.

The lock-in region in which the amplitude rises as a consequence of internal resonance between the wake oscillator and the structure is clearly seen in the figure about $U_r = 5$. It can be observed that the amplitude rises by a factor of approximately 20 about this value. This will lead to catastrophic results which need to be addressed, especially if the range of operation of the system falls around this value.

For this purpose, we introduce parametric excitation in structural stiffness. The governing equation of motion then becomes

$$\ddot{y} + \left(2\zeta\delta + \frac{\gamma}{\mu}\right)\dot{y} + \delta^2(1 + \alpha\cos\omega t)y = Mq \tag{3}$$

$$\ddot{q} + \varepsilon \left(q^2 - 1\right)\dot{q} + q = A\ddot{y} \tag{4}$$

We introduce the parameter $r=\frac{\omega}{\delta}$ which is the ratio between the parametric excitation frequency and the natural frequency of the structure. The vibration attenuation due to parametric excitation is studied based on this parameter. Figure 2 shows the variation of structural amplitude as a function of U_r for parametric excitation amplitude $\alpha=0.5$ and frequency ratio r=0.145. It is clear from the figure that the amplitude in the lock-in region is suppressed by a factor of 4. Although the parametric excitation introduces new lock-in regions either side of the original lock-in region, it is possible to push these regions out of the original lock-in region by adjusting the value of α and r.

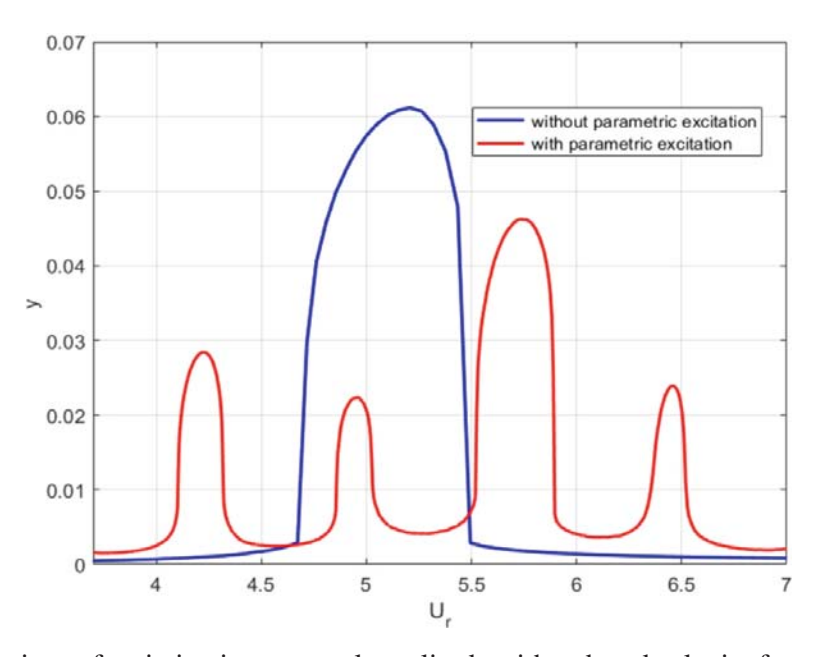


Fig. 2. Comparison of variation in structural amplitude with reduced velocity for systems without and with parametric excitation.

Figure 3 shows the comparison of amplitudes with and without parametric excitation for the case presented in Fig. 2, at $U_r = 5$.

The mitigation effect of parametric excitation can be enhanced by tuning the value of the frequency ratio r. Figure 4 shows the case of vibration mitigation at $U_r = 5$ and r = 0.943. It is seen that this frequency ratio gives far better mitigation than the previous one. Figure 4 clearly shows that parametric excitation may be used as a control strategy in self-excited systems with good effect.

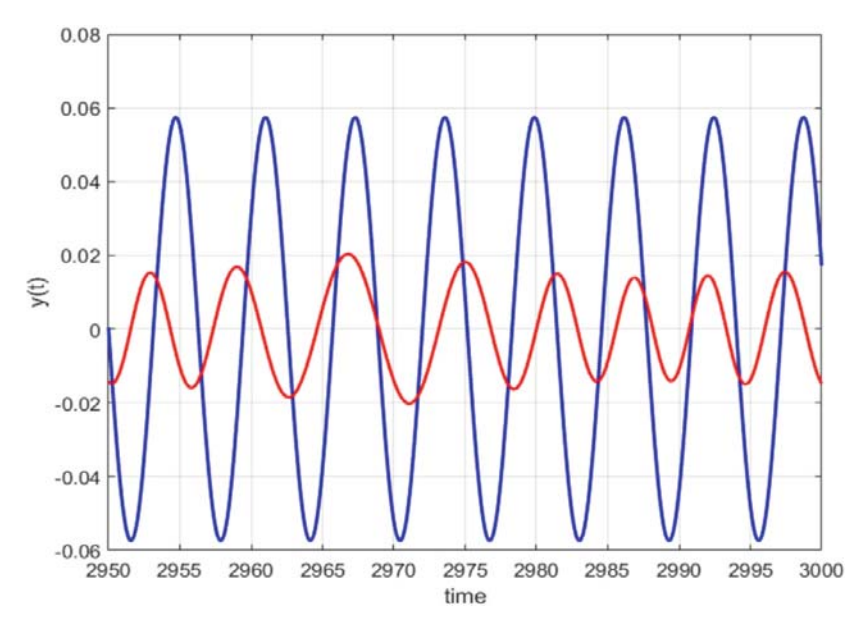


Fig. 3. Suppression of vibration amplitude in the lock-in region at $U_r = 5$. Blue curve for the system without parametric excitation and red line for that with parametric excitation.

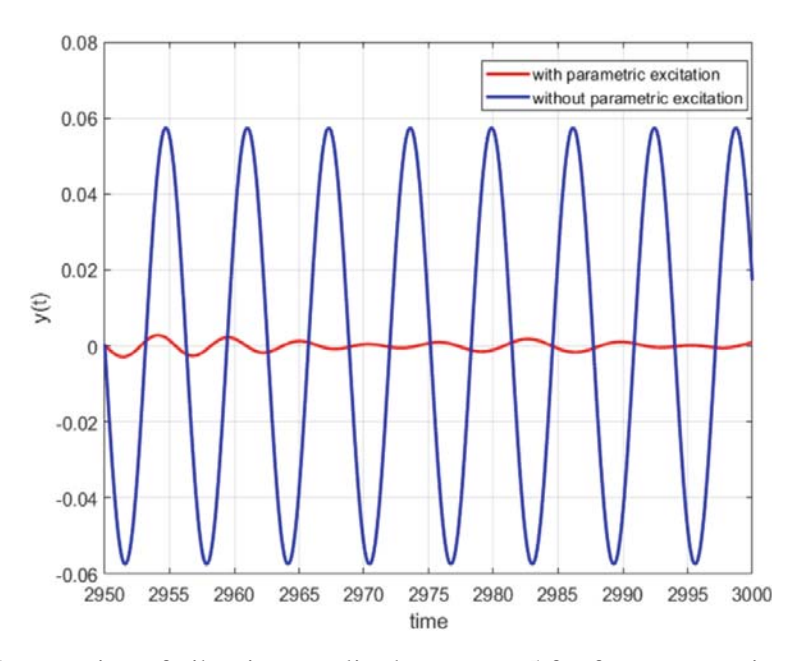


Fig. 4. Suppression of vibration amplitude at $U_r = 5$ for frequency ratio r = 0.943.

3 Control of Flow Induced Vibration Using Bistable Nonlinear Energy Sink

Different designs of NES have been used to suppress flow induced vibration [12, 13]. The present authors have recently demonstrated [19] the use of BNES to control flow induced vibration. The BNES is connected to the structure and its parameters are tuned so as to suppress the vibration imparted to the structure by the wake oscillations. The governing equations of the model in non-dimensional form are given by

$$(1 - \beta)\eta_1'' + 2\zeta\omega\eta_1' - 2\zeta_{nes}\omega(\eta_2' - \eta_1') - \alpha(\eta_2 - \eta_1) + \omega^2\eta_1 - \omega^2\gamma_{nes}(\eta_2 - \eta_1)^3 = ql - \Gamma\eta_1'$$
 (5)

$$\beta \eta_2'' - 2\zeta_{nes}\omega (\eta_1' - \eta_2') + \alpha(\eta_2 - \eta_1) - \gamma_{nes}\omega^2 (\eta_1 - \eta_2)^3 = 0$$
 (6)

$$q'' + \lambda (q^2 - 1)q' + q = P\eta_1''$$
 (7)

Here, η_1 , η_2 and q are the non-dimensional displacements of primary structure, BNES and wake oscillator, respectively. The non-dimensional parameters occurring in the equation are: β is the mass of BNES, ζ and ω are the damping and natural frequency of the structure respectively, q is the coupling coefficient between the wake and the structure, Γ is the lift coefficient, ζ_{nes} , α and γ_{nes} are viscous damping, linear and nonlinear stiffness coefficients of BNES, λ is the strength of nonlinearity of the wake oscillator and P is the acceleration coupling coefficient.

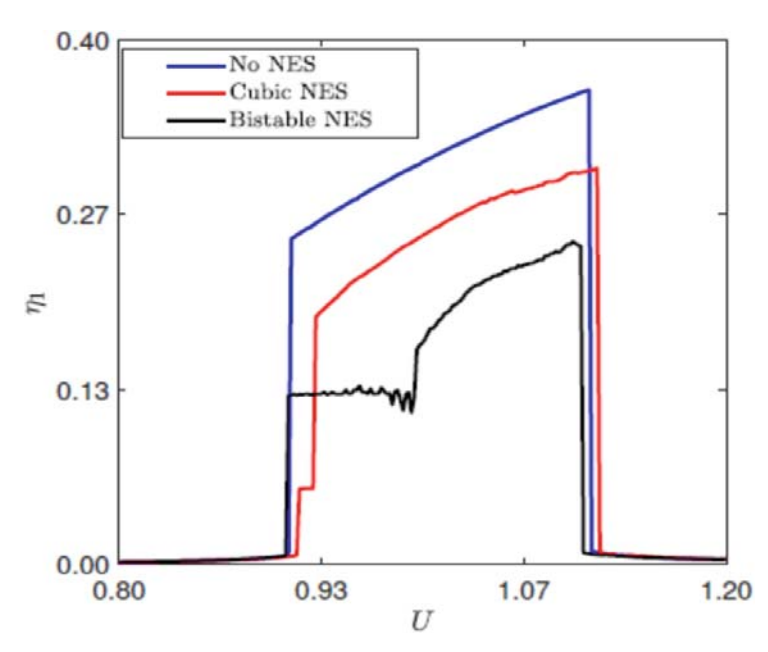


Fig. 5. Mitigation of amplitude of the structure by the use of BNES with non-dimensional mass $\beta = 0.01$. Reprinted with permission from [19]. © 2025, Elsevier B.V. All rights are reserved.

Figure 5 shows the comparison of structure amplitude with no NES, with cubic NES attached to the structure and with BNES attached. Other parameters are kept the same for comparison. It is clear that BNES causes considerable suppression of the structure amplitude and outperforms pure cubic NES. Two regimes are observed in Fig. 5 for structure amplitude when connected to BNES. To further analyse the partition of the lick-in region in the case of BNES, we plot the Poincare points and largest Lyapunov exponent for the same range of *U* in Fig. 6.

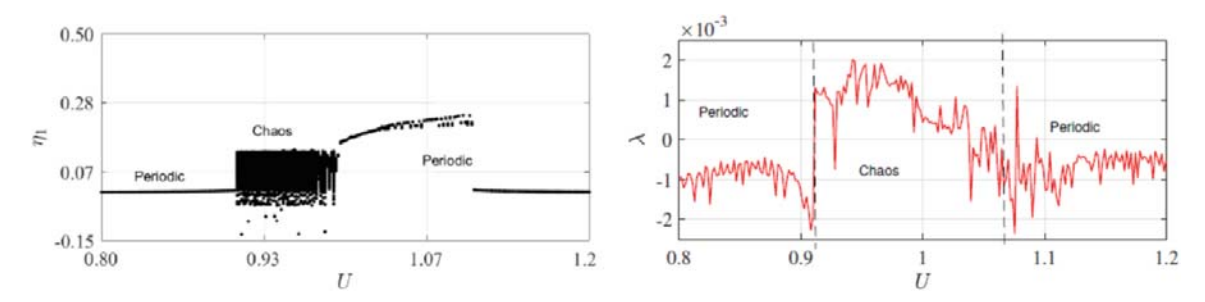


Fig. 6. Dynamic behaviour of the structure as reduced velocity U is varied in the range [0.8, 1.2]. Reprinted with permission from [19]. © 2025, Elsevier B.V. All rights are reserved.

Figure 6 shows that the lower branch of amplitudes shown in Fig. 5 is associated with chaotic solution. This solution branch bifurcates into a periodic one inside the lock-in region itself. But the amplitude of this periodic branch is significantly lesser than the original resonant amplitude and the amplitude obtained by using cubic NES. This shows that BNES is an efficient strategy to mitigate high amplitude flow induced vibrations in the lock-in region.

4 Control of Stick-Slip Vibrations in a Disc Brake Model

Control of stick-slip oscillations in self-excited non-smooth systems may be accomplished by the use of small amplitude normal excitation to the mass [20]. This may be demonstrated in a non-smooth disc brake model with three degrees of freedom shown in Fig. 7. Mass m_1 models the rotating disc, whereas m_2 models the brake calliper. The brake pad in contact with the rotating disc during the braking process is modelled by mass m_3 . The brake pad undergoes stick-slip oscillation in contact which is to be mitigated by the application of normal force $F_0 \cos \Omega t$ to the brake pad.

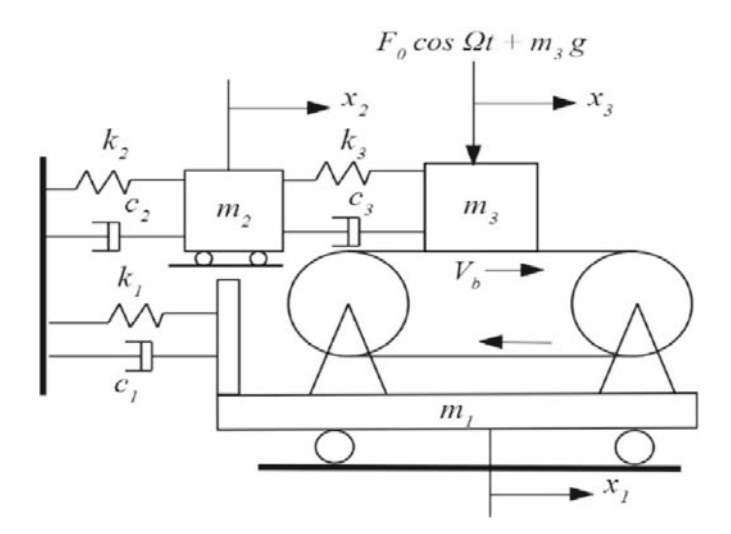


Fig. 7. Three degrees of freedom non-smooth model of a disc brake. Reprinted with permission from [20]. © 2025, Elsevier B.V. All rights are reserved.

The governing equations of the model are given by

$$m_1\ddot{x}_1 + c_1\dot{x}_1 + k_1x_1 = F_f \tag{8}$$

$$m_2\ddot{x}_2 + (c_2 + c_3)\dot{x}_2 - c_3\dot{x}_3 + (k_2 + k_3)x_2 - k_3x_3 = 0$$
(9)

$$m_3\ddot{x}_3 - c_3\dot{x}_2 + c_3\dot{x}_3 - k_3x_2 + k_3x_3 = -F_f \tag{10}$$

Here, F_f is the frictional force between the brake pad and the disc and is governed by $F_f = \mu(v_r)(m_3g + F_0\cos\Omega t)$, where μ is the coefficient of friction which is a function of the relative velocity v_r . It thus emerges that the normal force modulates the frictional force acting between the mass and the disc and causes a situation similar to that of parametric excitation. We consider Stribeck frictional model in the present case according to which

$$\mu(v_r) = \mu_s sgn(v_r) - \gamma_1 v_r + \gamma_3 v_r^3 \tag{11}$$

The relative velocity is given by $v_r = \dot{x}_3 - \dot{x}_1 - v_b$.

Figure 8 shows the state space of mass m_3 corresponding to the brake pad. Orbits corresponding to different values of non-dimensionalised forcing frequency ω are shown in the figure. It is observed that for larger value of frequency, the width of the sticking region is significant, which leads to prominent stick-slip orbits. But when the forcing frequency reaches $\omega \approx 1.4$, the orbit starts transversally intersecting the surface of discontinuity. This is due to switching-sliding bifurcation [20] which leads to the decrease in the sticking portion of the orbit. As the frequency is still reduced, we can see from the figure that the sticking portion of the orbit is significantly reduced. This leads to the suppression of stick-slip vibrations. It is thus clear that the normal force on the brake pad which causes modulation in the frictional force may be used to mitigate stick-slip oscillations.

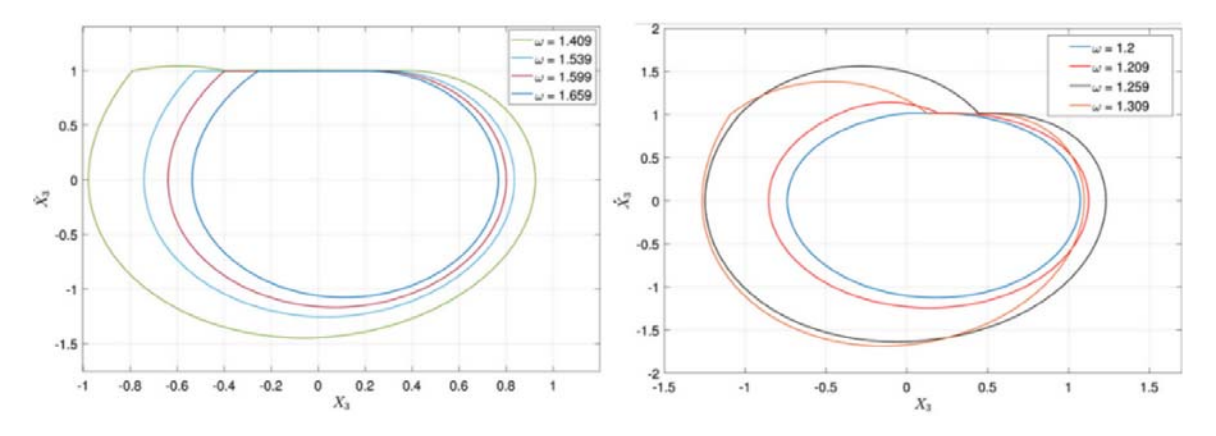


Fig. 8. Suppression of stick-slip oscillation by varying the frequency of the normal force applied to the brake pad. Reprinted with permission from [20]. © 2025, Elsevier B.V. All rights are reserved.

5 Conclusions

This article outlined the use of parametric and external excitation to mitigate self-excited vibrations in smooth and non-smooth systems. It also dealt with the use of BNES to suppress flow-induced vibration. Parametric excitation comes across as a very efficient method for the mitigation of self-excited systems. It was seen that the introduction of parametric excitation leads to newer internal resonance regions on both sides of the original lock-in region. Nevertheless, preliminary results are still very encouraging as it is possible to push these resonance peaks outside the original lock-in region. This leads to the suppression of amplitude in the lock-in region. The use of BNES, coupled to the structure, also gives good vibration suppression performance inside the lock-in region. It easily outperforms cubic NES in amplitude mitigation. It was also seen that BNES coupled structure partitions the lock-in region into a chaotic and non-chaotic one. Normal harmonic external excitation was seen to be successful in suppressing the stickslip vibrations in the disc brake model. The external excitation modulates the frictional force and bring about a situation similar to parametric excitation. Switching-sliding bifurcation is what causes the decrease in the width of the sticking region which in turn leads to suppression of stick-slip oscillation.

Acknowledgements. This work has been supported by the Polish National Science Centre, Poland under the grant OPUS 26 No. 2023/51/B/ST8/00021.

References

- 1. Van der Pol, B., van der Mark, J.: The heartbeat considered as a relaxation oscillation, and an electrical model of the heart. Philos. Mag. **6**(7), 763–775 (1928)
- 2. Grudzinski, K., Zebrowski, J.J.: Modelling cardiac pacemakers with relaxation oscillators. Physica A **336**, 153–162 (2004)
- 3. Izhikevich, E.M.: Dynamical Systems in Neuroscience: The Geometry of Excitability and Bursting, 1st edn. MIT Press, Cambridge, MA (2007)
- 4. Fletcher, N.H., Rossing, T.D.: The Physics of Musical Instruments, 1st edn. Springer-Verlag, New York (1991)
- 5. Païdoussis, M.P., Price, S., de Langre, E.: Fluid-Structure Interactions: Cross-Flow-Induced Instabilities, 1st edn. Cambridge University Press, Cambridge (2011)
- 6. Chai, Y., Gao, W., Ankay, B., Li, F., Zhang, C.: Aeroelastic analysis and flutter control of wings and panels: a review. Int. J. Mechan. Sys. Dyn. 1, 5–34 (2021)
- 7. Merrit, H.E.: Theory of self-excited tool chatter: Research 1. ASME J. Eng. Indus. **87**, 447–454 (1965)
- 8. Pilipchuk, V., Olejnik, P., Awrejcewicz, J.: Transient friction-induced vibrations in a 2-DOF model of brakes. J. Sound Vib. **344**, 297–312 (2015)
- 9. Tondl, A.: On the interaction between self-excited and parametric vibrations. National Research Institute for Machine Design, Monograph No. 25, Bechovice, Prague (1978)
- 10. Nabergoj, R., Tondl, A.: Self-excited vibration quenching by means of parametric excitation. Acta Tech. CSAV **46**, 107–118 (2001)
- 11. Tondl, A.: To the problem of self-excited vibration suppression. Eng. Mech. **15**, 297–307 (2008)

- 12. Chirathalattu, A.T., Santhosh, B., Bose, C., Philip, R., Balaram, B.: Passive suppression of vortex-induced vibrations using a nonlinear energy sink Numerical and analytical perspective. Mech. Syst. Signal Process. **182**, 109556 (2023)
- 13. Philip, P., Santhosh, B., Balaram, B., Awrejcewicz, J.: Vibration control in fluid conveying pipes using NES with nonlinear damping. Mech. Syst. Signal Process. **194**, 110250 (2023)
- 14. Dohnal, F., Tondl, A.: Suppressing flutter vibrations by parametric inertia excitation. J. Appl. Mech. (2009)
- 15. Yao, Z., Mei, D., Chen, Z.: Chatter suppression by parametric excitation: Model and experiments. J. Sound Vib. **330**, 2995–3005 (2011)
- 16. Das, J., Mallik, A.K.: Control of friction driven oscillation by time-delayed state feedback. J. Sound Vib. **297**, 578–594 (2006)
- 17. Liu, N., Ouyang, H.: Suppression of friction-induced-vibration in MDoF systems using tangential harmonic excitation. Meccanica **55**, 1525–1542 (2020)
- 18. Facchinetti, M.L., de Langre, E., Biolley, F.: Coupling of structure and wake oscillators in vortex-induced vibrations. J. Fluids and Struct. **19**(2), 123–140 (2004)
- 19. Maity, S., Santhosh, B., Balaram, B., Awrejcewicz, J.: Suppression of vortex-induced vibrations using bistable nonlinear energy sink. Communications in Nonlinear Science and Numerical Simulation (in print)
- 20. Balaram, B., Santhosh, B., Awrejcewicz, J.: Frequency entrainment and suppression of stick—slip vibrations in a 3 DoF discontinuous disc brake model. J. Sound Vib. **538**, 117224 (2022)